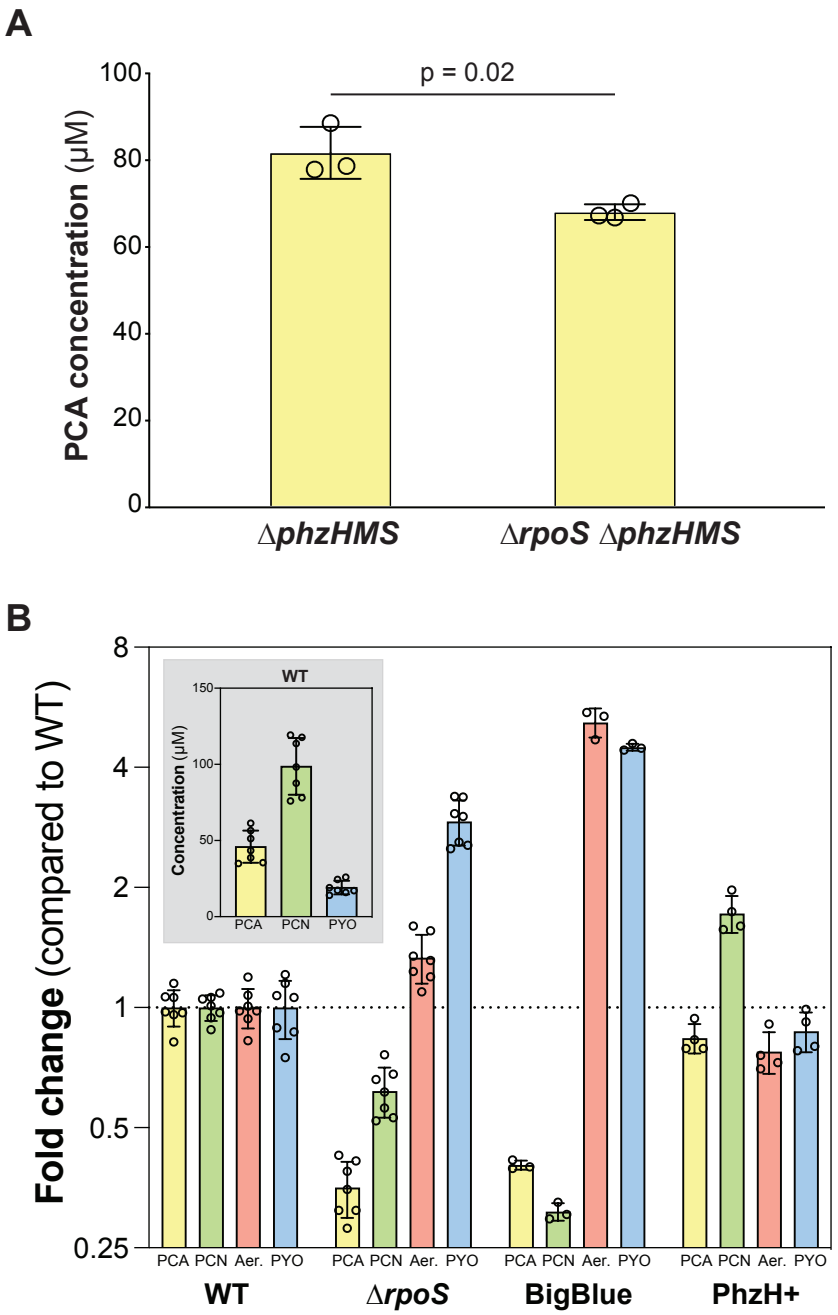

Figure S1. Quantification of phenazines from PA14 colony biofilms. (A) PCA produced by macrocolony biofilms of PA14 and Δ*rpoS* strains lacking *phzH, phzM,* and *phzS* (Δ*phzHMS*). In these strains, the PCA production is indicative of the total amount of phenazines made due to the lack of the phenazine modification enzymes. Data points represent biological triplicates and error bars represent standard deviation. The *p* value was calculated using an unpaired, two-tailed *t*-test. **(B)** Change in phenazine production by Δ*rpoS*, BigBlue, and PhzH+ biofilms relative to biofilms formed by WT PA14. Inset: absolute values of phenazines in a WT biofilm. Macrocolony biofilms were grown on 1% tryptone, 1% agar for 72 hours. Aer., aeruginosins. Individual points represent biological replicates and error bars represent standard deviation.

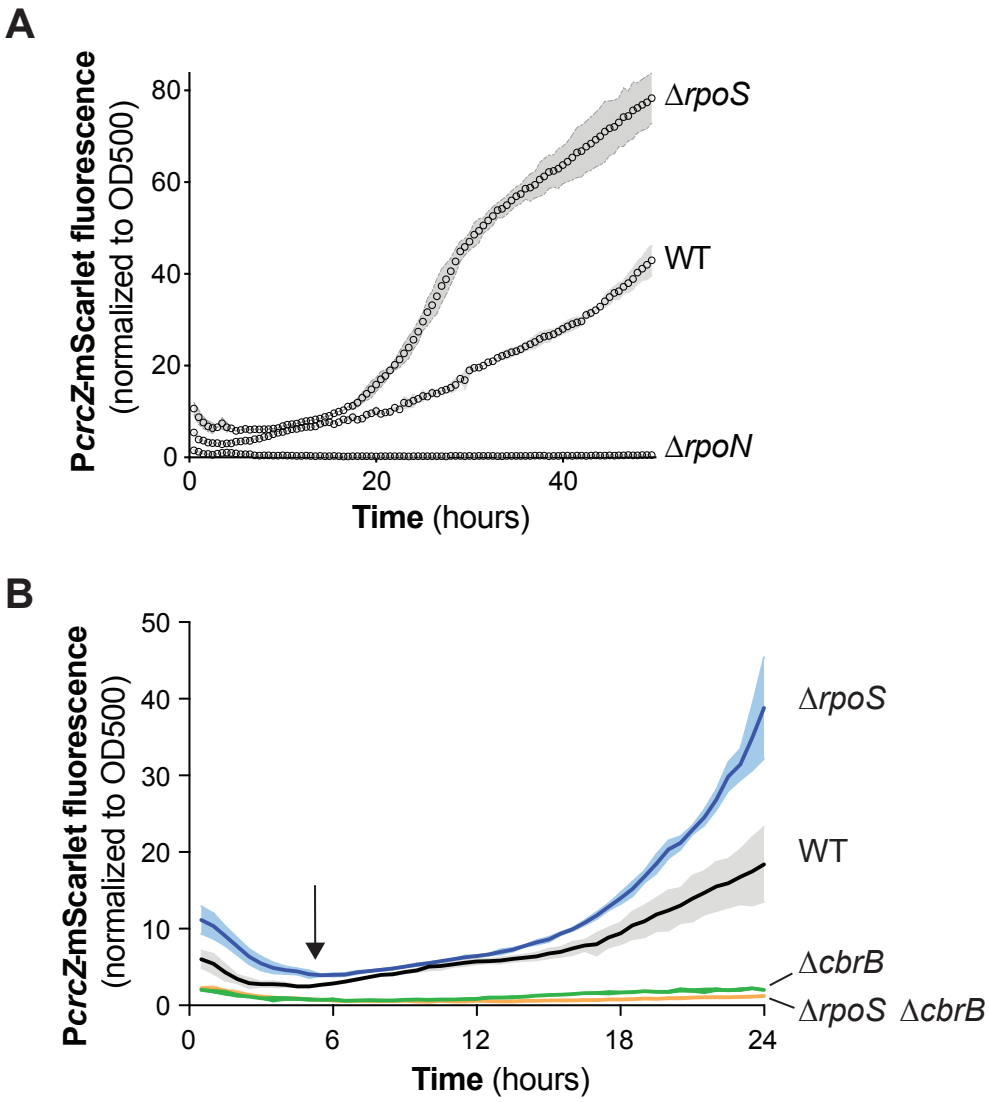

Figure S2. Deletion of *cbrB* abrogates *crcZ* expression in the Δ*rpoS* background. (**A**) PA14, Δ*rpoS*, Δ*rpoN* strains with P*crcZ-mScarlet* were grown in 1% tryptone broth with shaking for 24 hours. (**B**) PA14, Δ*rpoS,* Δ*cbrB,* and Δ*rpoS*Δ*cbrB* strains were grown in 1% tryptone broth with shaking for 24 hours. The arrow indicates the onset of stationary phase. Traces represent the averages of biological triplicates and shading indicates standard deviation.

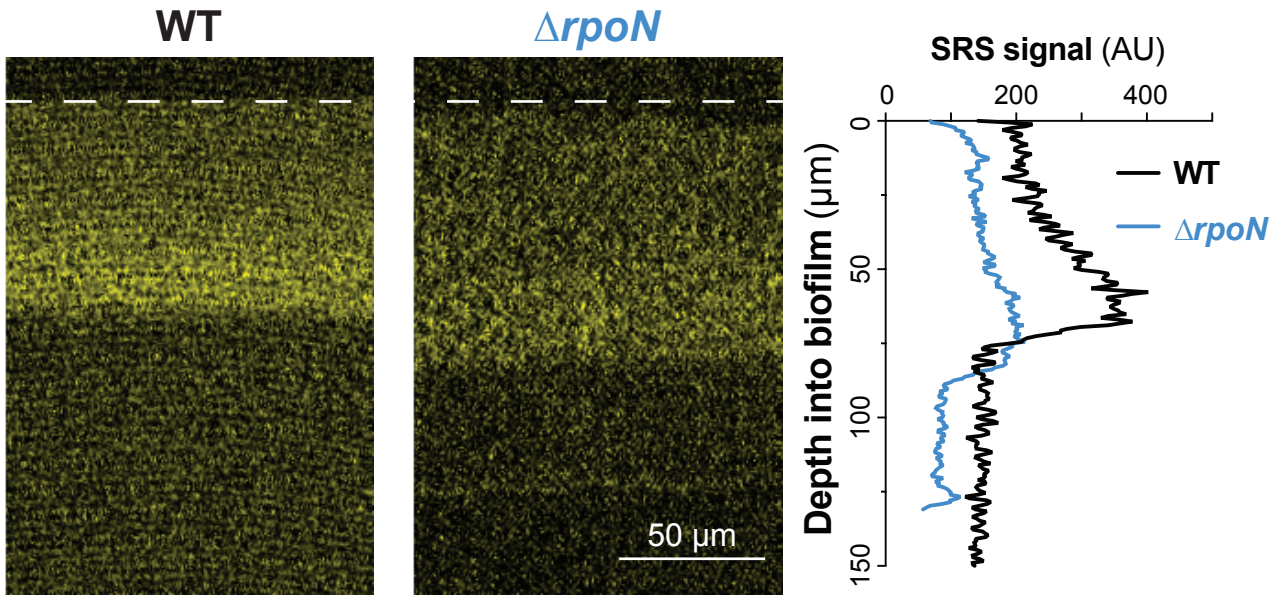

Figure S3. The effect of RpoN on biofilm metabolic activity is consistent with its role in *crcZ* expression. Left and center: SRS images of thin sections prepared from WT and Δ*rpoN* biofilms. SRS signal is indicative of metabolic activity and is false-colored yellow. Right: Average SRS signal across depth. The experiment was performed in biological triplicate and representative images are shown.

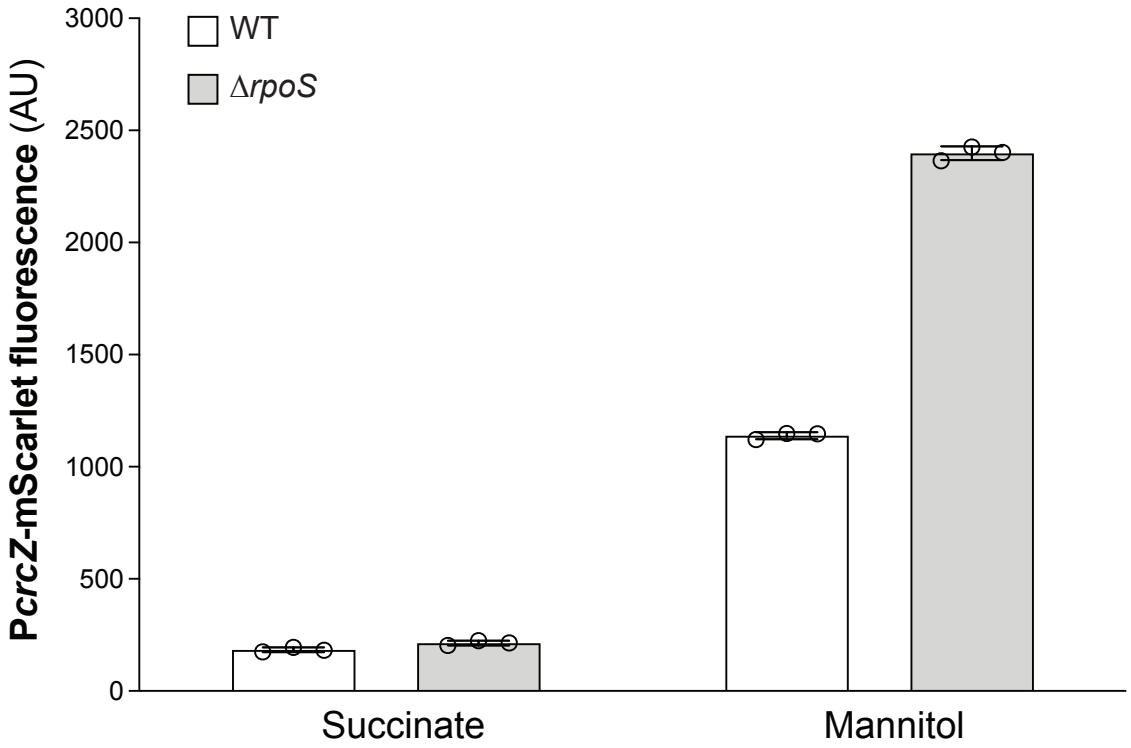

Figure S4. *rpoS* deletion enhances *crcZ* expression during liquid-culture growth on mannitol, a nonpreferred carbon source. The WT and Δ*rpoS* P*crcZ-mScarlet* reporter strains were grown in a defined medium to an OD (500 nm) of 0.3 with the indicated compounds as sole carbon sources. Individual points represent biological triplicates and error bars represent standard deviation.

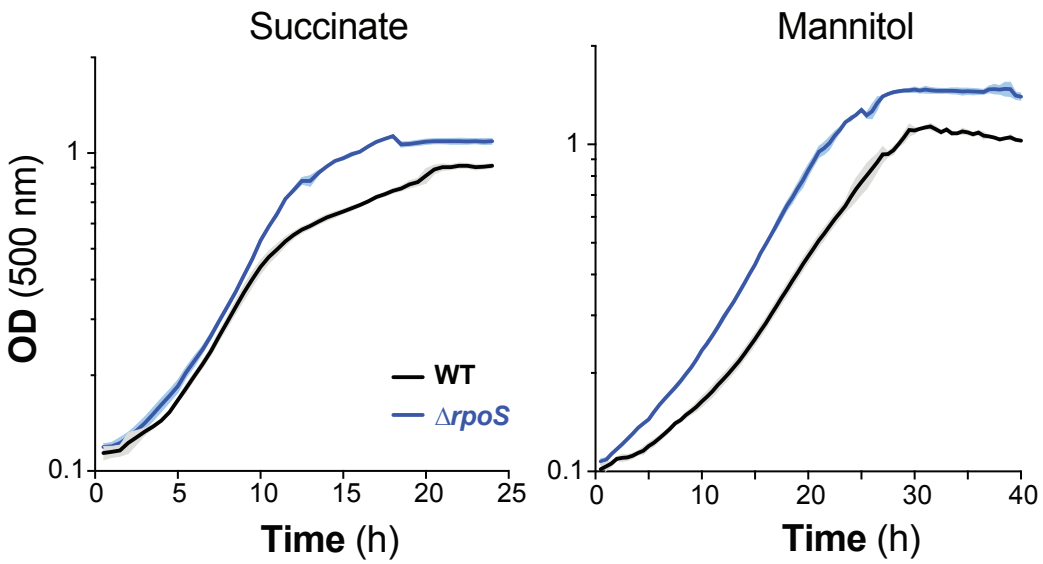

Figure S5. Effects of *rpoS* and *crc* deletions on planktonic growth with individual carbon sources. PA14 and Δ*rpoS* were grown in a defined medium with 20 mM succinate or mannitol. Traces represent the averages of biological triplicates and shading indicates standard deviation. Mannitol cultures were grown for 40 hours to capture the complete growth cycle.

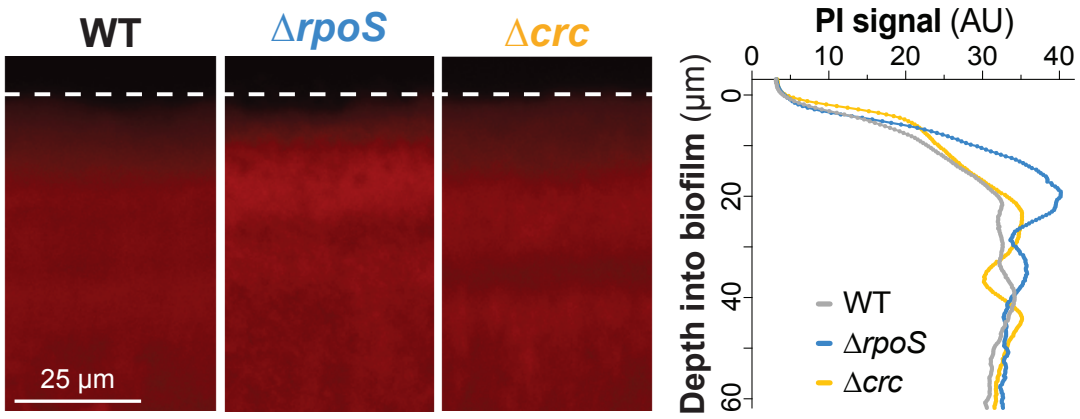

Figure S6. Propidium iodide staining reveals increased death at the biofilm-air interface Δ*rpoS* biofilms. Fluorescence images of thin sections prepared from WT, Δ*rpoS*, and Δ*crc* biofilms. Biofilms were grown on 1% tryptone, 1% agar for 72 hours then transferred to equivalent medium containing 50 μM propidium iodide for 6 hours. Right: Average propidium iodide signal across depth. The experiment was performed in biological triplicate and representative images are shown.

Table S1. Bacterial strains used in this study.

Number	Strain	Description	Source
Pseudomonas aeruginosa strains			
LD0	UCBPP-PA14 (WT)	Clinical isolate UCBPP-PA14	(1)
LD24	Δ*phz* (also referred to as Δ*phz1/2*)	PA14 with the *phzA1-G1* (*PA14_09480-PA14_09410*) and *phzA2-G2* (*PA14_39970-PA14_39880*) operons deleted	(2)
LD3692	Δ*phzH*	PA14 with *phzH* (*PA14_00640*) deleted	(3)
LD3739	Δ*phzMS*	PA14 with *phzM* (*PA14_09490*) and *phzS* (*PA14_09400*) deleted	(3)
LD3746	Δ*phzHMS*	PA14 with *phzH* (*PA14_00640*), *phzM* (*PA14_09490*), and *phzS* (*PA14_09400*) deleted	(4)
LD851	Δ*phzHS*	PA14 with *phzH* (*PA14_00640*) and *phzS* (*PA14_094400*) deleted	(3)
LD64	BigBlue (*phzM+)*	DKN370; PA14 merodiploid strain containing an extra copy of *phzM* (*PA14_09490*)	(5)
LD3192	Δ*rpoS*	PA14 with *rpoS* (*PA14_17480*) deleted	This study
LD3193	Δ*rpoS*Δ*phz*	PA14 with *rpoS* (*PA14_17480*) and the *phz1* (*PA14_09480-PA14_09410*) and *phz2* (*PA14_39970-PA14_39880*) operons deleted	This study
LD3469	Δ*rpoS*Δ*phzHMS*	PA14 with *rpoS* (*PA14_17480*), *phzH* (*PA14_00640*), *phzM* (*PA14_09490*), and *phzS* (*PA14_09400*) deleted	This study
LD3674	Δ*crc*	PA14 with *crc* (*PA14_70390*) deleted	This study
LD3675	Δ*crc*Δ*phz*	PA14 with *crc* (*PA14_70390*) and the *phz1* (*PA14_09480-PA14_09410*) and *phz2* (*PA14_39970-PA14_39880*) operons deleted	This study
LD3717	Δ*rpoS*Δ*crc*	PA14 with *rpoS* (*PA14_17480*) and *crc* (*PA14_70390*) deleted	This study
LD3190	Δ*rpoN*	PA14 with *rpoN* (*PA14_57940*) deleted	This study

LD4497	Δ*cbrB*	PA14 with *cbrB* (*PA14_62540*) deleted	This study
LD4500	Δ*rpoS*Δ*cbrB*	PA14 with *rpoS* (*PA14_17480*) and *cbrB* (*PA14_62540*) deleted	This study
LD5068	PA14 attTn7::PPA1/04/03-PhzH	PA14 containing a construct in the attTn7 site that expresses the coding region of PhzH under control of the lac-derived constitutive PA1/04/03 promoter.	This study
LD3870	PA14 attB::P*crc-mScarlet*	PA14 containing a construct in the *attB* site that expresses *mScarlet* under control of the 500bp region upstream of *crc* (*PA14_17480)*	This study
LD4082	PA14 attB::P*crcZ-mScarlet*	PA14 containing a construct in the *attB* site that expresses *mScarlet* under control of the 350bp region upstream of *crcZ* (Unannotated between *PA14_62540* and *PA14_62560*. Annotated as *PA4726.11* in PAO1)	This study
LD3941	Δ*rpoS* attB::P*crc-mScarlet*	Δ*rpoS* (*PA14_17480*) containing a construct in the *attB* site that expresses *mScarlet* under control of the 500bp region upstream of *crc* (*PA14_17480)*	This study
LD4108	Δ*rpoS* attB::P*crcZ-mScarlet*	Δ*rpoS* (*PA14_17480*) containing a construct in the *attB* site that expresses *mScarlet* under control of the 350bp region upstream of *crcZ* (Annotated as *PA4726.11* in PAO1)	This study
LD4498	Δ*cbrB* attB::P*crcZ-mScarlet*	PA14 attB::P*crcZ-mScarlet*, with *cbrB* (*PA14_62540)* deleted	This study
LD4501	Δ*rpoS*Δ*cbrB* attB::P*crcZ-mScarlet*	PA14 attb::P*crcZ-mScarlet*, with *cbrB* (*PA14_62540)* and *rpoS* (*PA14_17480*) deleted	This study
LD4229	Δ*rpoN* attB::P*crcZ-mScarlet*	PA14 attb::P*crcZ-mScarlet*, with *rpoN* (*PA14_57940*) deleted	This study
E. coli strains			
LD44	UQ950	E. coli DH5α λ(pir) host for cloning; F-Δ(*argF-lac*)169 Φ80 d*lacZ58*(ΔM15) *glnV44*(AS) *rfbD1 gyrA96*(NalR) *recA1 endA1 spoT1 thi-1 hsdR17 deoR* λpir+	D. Lies
LD661	BW29427	Donor strain for conjugation: *thrB1004*	W. Metcalf

		pro thi rpsL hsdS lacZ ΔM15RP4–1360 Δ(*araBAD*)567 Δ*dapA1341*::[*erm pir*(wt)]	
LD2901	S17-1	Donor strain for conjugation: Str^R, Tp^R, F^- RP4-2-Tc::Mu *aphA*::Tn7 *recA* λpir lysogen	R. Simon
Saccharomyces cerevisiae strains			
LD676	InvSc1	*MATα/MATα leu2/leu2 trp1-289/trp1-289 ura3-52/ura3-52 his3-Δ1/his3-Δ1*	Invitrogen

Table S2. Plasmids used in this study.

Plasmid Name	Description	Source
pMQ30	Yeast-based allelic-exchange vector; *sacB*$^+$, CEN/ARSH, URA3$^+$, Gm^R.	(6)
pFLP2	Site-specific excision vector with cl857-controlled FLP recombinase. encoding sequence, sacB$^+$, Amp^R. Used to insert LD3208-based plasmids into P. aeruginosa strains.	(7)
pLD3208	Gm^R, Tet^R flanked by Flp recombinase target (FRT) sites to resolve out resistance cassettes.	(8)
pAKN69	GmR, CmR mini-Tn7 PPA1/04/03::yfp	(9)
pLD3471	Δ*rpoS* (*PA14_17480*) PCR fragment introduced into pMQ30 by gap repair cloning in yeast strain InvSc1.	This study
pLD3473	Δ*rpoN* (*PA14_57940*) PCR fragment introduced into pMQ30 by gap repair cloning in yeast strain InvSc1.	This study
pLD3673	Δ*crc* (*PA14_70390*) PCR fragment introduced into pMQ30 by gap repair cloning in yeast strain InvSc1.	This study
pLD5056	Δ*cbrB* (*PA14_62540*) PCR fragment introduced into pMQ30 by gap repair cloning in yeast strain InvSc1.	This study
pLD5065	The CDS of PhzH (*PA14_00640*) with lambda t0 terminator PCR fragment ligated into pAKN69 using NheI and SphI.	This study
pLD3869	500 bp upstream of *crc* (*PA14_70390*) PCR fragment ligated into pLD3208 using SpeI and XhoI.	This study
pLD4645	350 bp upstream of *crcZ* (annotated as *PA4726.11* in PAO1) PCR fragment ligated into pLD3208 using SpeI and XhoI.	This study

Table S3. Primers used in this study.

Primer Number	Sequence
Primers for plasmid pLD3471 (used to make Δ*rpoS*)	
LD2560	ggaattgtgagcggataacaatttcacacaggaaacagct TGGATAAGGGGGAAGGATTG
LD2561	CCGTTCTTCTCCAGGATCTC CGGCCCTTCTTTTTTGAGTGC
LD2562	GCACTCAAAAAAGAAGGGCCG GAGATCCTGGAGAAGAACGG
LD2563	aggcaaattctgttttatcagaccgcttctgcgttctgat AAACCACCAGCCTGCCGCAC
Primers for plasmid pLD3473 (used to make Δ*rpoN*)	
LD2568	ggaattgtgagcggataacaatttcacacaggaaacagct CGCGCCCGCGCATCGACATG
LD2569	CACCAGTCGCTTGCGCTC CATCTTGAGGACTAGCGATGG
LD2570	CCATCGCTAGTCCTCAAGATG GAGCGCAAGCGACTGGTG
LD2571	aggcaaattctgttttatcagaccgcttctgcgttctgat CAGGGCGCGCTGCGCCAGGT
Primers for plasmid pLD3673 (used to make Δ*crc*)	
LD3184	ggaattgtgagcggataacaatttcacacaggaaacagct GCCCTTGTCGTTGACGTAGC
LD3185	TCGACGATCAGCGGCGCATGC CCGCAGCCTGAATACCATTCAC
LD3186	GTGAATGGTATTCAGGCTGCG GCATGCGCCGCTGATCGTCGA
LD3197	aggcaaattctgttttatcagaccgcttctgcgttctgatTCGGCGAGAACACCCTGTAC
Primers for plasmid pLD5056 (used to make Δ*cbrB*)	
LD4030	ggaattgtgagcggataacaatttcacacaggaaacagct CTGGTGCTACTGGTGGAAG
LD4031	GAAAGGTCCTCGGTGGGCTC GGTTTCGTCTTCGACGATCA
LD4032	TGATCGTCGAAGACGAAACC GAGCCCACCGAGGACCTTTC
LD4033	aggcaaattctgttttatcagaccgcttctgcgttctgat GTCTGCGCGGATTCTAGCAT
Primers for plasmid pLD5065 (used to make PhzH+)	

LD4528	gattcgactgc gcatgctgTGCGGTCTCGCGGG
LD4529	actggatctatcaacaggagtccaaTCAGGCGGAGAGCCC
LD4530	CAGGTTGTACGGGCTCTCCGCCTGAttggactcctgttgatagatccag
LD4077	acgtacgtacgctagcTTGGATTCTCACCAATAAAAAACGCC
Primers for plasmid pLD3869 (used to make *Pcrc-mScarlet*)	
LD3273	tcccgacgggcccggtaccaGATGATCTGCATCACTTCG
LD3274	tcttaaatctagactcgaggAAATGGCCCCCAAAATCAC
Primers for plasmid pLD4645 (used to make *PcrcZ-mScarlet*)	
LD3663	acgtacactagtCACCCTGCAACCTGTTACC
LD3272	tcttaaatctagactcgaggCAATACATAAGCAGATGCCGTGCC

Supplementary references

1. L. G. Rahme, *et al.*, Common virulence factors for bacterial pathogenicity in plants and animals. *Science* **268**, 1899–1902 (1995).

2. L. E. P. Dietrich, A. Price-Whelan, A. Petersen, M. Whiteley, D. K. Newman, The phenazine pyocyanin is a terminal signalling factor in the quorum sensing network of Pseudomonas aeruginosa. *Mol. Microbiol.* **61**, 1308–1321 (2006).

3. D. L. Bellin, *et al.*, Integrated circuit-based electrochemical sensor for spatially resolved detection of redox-active metabolites in biofilms. *Nat. Commun.* **5**, 3256 (2014).

4. D. A. Recinos, *et al.*, Redundant phenazine operons in Pseudomonas aeruginosa exhibit environment-dependent expression and differential roles in pathogenicity. *Proc. Natl. Acad. Sci. U. S. A.* **109**, 19420–19425 (2012).

5. A. Price-Whelan, L. E. P. Dietrich, D. K. Newman, Pyocyanin alters redox homeostasis and carbon flux through central metabolic pathways in Pseudomonas aeruginosa PA14. *J. Bacteriol.* **189**, 6372–6381 (2007).

6. R. M. Q. Shanks, N. C. Caiazza, S. M. Hinsa, C. M. Toutain, G. A. O'Toole, Saccharomyces cerevisiae-based molecular tool kit for manipulation of genes from gram-negative bacteria. *Appl. Environ. Microbiol.* **72**, 5027–5036 (2006).

7. T. T. Hoang, R. R. Karkhoff-Schweizer, A. J. Kutchma, H. P. Schweizer, A broad-host-range Flp-FRT recombination system for site-specific excision of chromosomally-located DNA sequences: application for isolation of unmarked Pseudomonas aeruginosa mutants. *Gene* **212**, 77–86 (1998).

8. B. Wang, *et al.*, Pseudomonas aeruginosa PA14 produces R-bodies, extendable protein

polymers with roles in host colonization and virulence. *Nat. Commun.* **12**, 4613 (2021).

9. L. Lambertsen, C. Sternberg, S. Molin, Mini-Tn7 transposons for site-specific tagging of bacteria with fluorescent proteins. *Environ. Microbiol.* **6**, 726–732 (2004).